Macromolecular Materials and Engineering
Open Access
www.mame-journal.de

Innovative Thermosensitive Composite Materials: Merging Poloxamer PF-127 and Polysaccharides for Enhanced Functional Properties

Marcos Blanco-López, Inmaculada de Dios-Pérez, Álvaro González-Garcinuño, Antonio Tabernero, and Eva Martín del Valle*

Currently, new cancer treatment options are being developed following tumor resection surgery, with a focus on minimizing invasiveness and reducing systemic toxicity to lower the risk of recurrence. In this context, the thermosensitive poloxamer Pluronic Acid F-127 (PF-127) is modified by incorporating polysaccharides with varying structures—xanthan gum (XG), alginate (ALG), gellan gum (GG), and levan (LEV). Hydrogels are synthesized using different ratios of polysaccharides and PF-127. Rheological results reveal that adding polysaccharides to the hydrogel matrix increases storage moduli from 8 to 11–18 kPa and viscosity from 4.5 to 6.1–7.1 Pa s. Additionally, the micellar aggregation capacity (MAC) and gelation temperature shift from 34 °C to between 22 and 31 °C. Studies on 5-fluorouracil (5-FU) release from these composites indicate that enhanced MAC prolongs drug release 4 times longer compared to the hydrogel made with PF-127 alone. A mathematical model is applied to analyze these experimental results, taking into account polymer chain release. Hydrogel's degradation rate and viscosity are primary determinants of drug release duration. Thus, by modifying the hydrogel composition, MAC, thermosensitivity, and drug release profile can be finely controlled based on the polysaccharide used.

1. Introduction

Cancer remains a significant medical and societal burden, posing an ongoing challenge for healthcare and scientific research. In particular, breast cancer's high heterogeneity complicates treatment strategies, since conventional therapies, like radiotherapy and chemotherapy, are often associated with severe side effects and systemic toxicity that also impact healthy breast tissue cells.[1] To improve efficacy, selectivity, and patient quality of life, research is increasingly directed toward developing personalized and more effective therapies.

In cases requiring tumor resection, current surgical techniques aim for minimal invasiveness to preserve surrounding healthy tissue. Adjuvant therapies, including immunotherapy and targeted therapy, focus on selectively eliminating residual cancer cells while safeguarding healthy cells in the peritumoral region.[2]

One promising approach in personalized treatment strategies involves alternative methods of drug delivery post-tumor removal, using advanced localized drug delivery systems. Such localized delivery is particularly advantageous in breast cancer treatment, as it provides sustained release of therapeutic agents directly at the tumor site, reducing unwanted systemic distribution and thus minimizing the risk of recurrence.[2]

Biocompatible compounds are at the forefront of these alternative treatment systems, acting as drug delivery systems (DDSs). The primary DDS options being explored include liposomes, nanoparticles, and hydrogels. Among these, hydrogels offer unique advantages: they have the potential for stimulus-responsive synthesis, and can fill tissue cavities, serving as matrices for embedding additional therapeutic particles.[3–5]

Hydrogels have long demonstrated versatile applications, especially in tissue engineering,[6] cell growth matrices,[7] and drug encapsulation and delivery.[8] For drug delivery, hydrogels offer significant potential for localized breast cancer treatment, particularly after tumor resection, as they allow for drug protection, targeting, and efficient encapsulation.[9] Postresection, the hydrogel can be directly injected into the cavity, aiming to prevent recurrence through a more precise delivery method that minimizes harm to healthy cells and systemic toxicity.[10] Moreover, injectable hydrogels for localized drug delivery provide several advantages over conventional methods like oral or intravenous

M. Blanco-López, I. de Dios-Pérez, Á. González-Garcinuño, A. Tabernero, E. Martín del Valle
Department of Chemical Engineering
University of Salamanca
Plaza Los Caídos s/n, Salamanca 37008, Spain
E-mail: antaber@usal.es
Á. González-Garcinuño, A. Tabernero, E. Martín del Valle
Institute for Biomedical Research in Salamanca (IBSAL)
Paseo de San Vicente 87, Salamanca 37007, Spain
The ORCID identification number(s) for the author(s) of this article can be found under https://doi.org/10.1002/mame.202400457

DOI: 10.1002/mame.202400457

delivery, which often suffer from low bioavailability and lack target specificity.[11]

This localized approach positions the drug close to the lesion, preventing local relapse of breast tumors after breast-conserving therapy.[12] Consequently, it offers a promising alternative focused on minimizing side effects and enhancing targeted drug delivery to cancerous cells.[2]

However, hydrogels often face limitations for injectability and initially rapid drug release, typically addressed by incorporating thermosensitivity to respond to temperature changes.[13] Thermosensitive injectable hydrogels have been explored in applications like DNA vaccine delivery,[14] bone regeneration,[15] wound healing, and cancer therapy.[16,17] For localized drug release, thermosensitive hydrogels are particularly valuable as they adapt to temperature variations, enabling controlled drug delivery and reducing the initial burst release.[10] Their aqueous, injectable form transitions to a gel state within the body, where they control release and fill cavities in a stable matrix, a key advantage for alternative treatments aimed at maximizing therapeutic efficiency.[18]

Thermosensitive hydrogels are also highly versatile, biocompatible, and biodegradable.[19] They undergo gelation at a specific transition temperature. This gelation process involves a shift from a liquid solution at room temperature (25 °C) to a gel at physiological temperature (37 °C) within the body.[20] This transition allows the gel to serve as a drug reservoir, gradually releasing the encapsulated agent at the injection site.[21]

A widely studied compound for thermosensitive hydrogel synthesis is Pluronic Acid F-127, or Poloxamer P407 (PF-127), a biocompatible, FDA-approved poloxamer capable of forming said hydrogels.[21] PF-127 is a nonionic surfactant composed of triblock polymers with two hydrophilic polyethylene oxide (PEO) ends and a hydrophobic polypropylene oxide (PPO) center. Concretely, it is a Pluronic (P) presented in flakes at room temperature (F) with a molecular weight of ≈12 600 g mol^{-1} (12), presenting the following structure: $(PEO)_{99}$–$(PPO)_{69}$–$(PEO)_{99}$. This structure determines a PPO/PEO ratio of ≈0.70 (7).[22]

The gelation transition of PF-127 falls within the target range for this application (25–37 °C), allowing the polymer micelles to gel through its micellar aggregation capacity (MAC) when heated, which leads to a stable hydrogel network as water evaporates.[23] Pluronic triblock copolymer structures present lipotropic and thermotropic behaviors. This means that PF-127 undergoes two different aggregation phenomena when in aqueous solution: micellization over the critical micellization temperature (cmt) when their concentration is higher than the minimum micellar concentration, and gellification, starting at critical gelation temperature (cgt) and stabilizing at the gelation completion temperature (gct).[24]

The transition from unimers to micelles comes from the dehydration of the PPO blocks, caused by an endothermic heat of micellization. After micellization, PF-127 has been reported to self-assembly in spherical micelles, since PEO/PPO ratio is higher than 0.5. The spherical micelles constitute a liotropic liquid phase (L_1) with isotropic behavior in aqueous solutions. Additionally, thermotropic behavior is expected. This implies that there is no need to increase the PF-127 concentration in order to appreciate a phase transition or structure reorganization, as presented in the phase diagram in **Figure 1**. When the temperature is increased, at a constant concentration, the spherical micelles undergo a first order transition by hard sphere interaction into a cubic phase (BCC) (Q_2) which is transparent, optically isotropic, highly viscous, and more elastic.[25] This cubic phase can present crystals when the concentration is closer to 100 wt%. Moreover, only a tight two-phase region is presented between the L_1 and the Q_2 phase, coinciding the MAC gelling transition. It must be noted that for other Pluronic compounds, such as P123, L122, or L121, this cubic phase is decreased in their diagram in order to promote the hexagonal or lamellar phase, due to the decrease of the PEO/PPO ratio.[25] Phase diagram for PF-127 is presented in Figure 1 below.

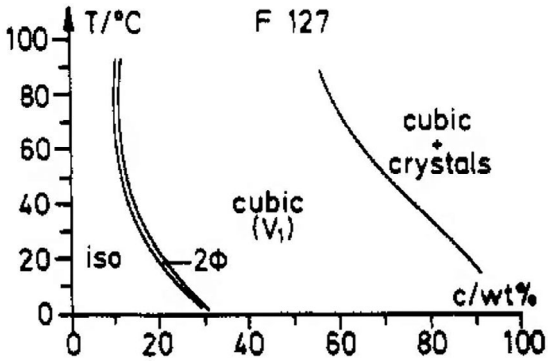

Figure 1. Phase diagram of PF-127. Reproduced with permission.[25] Copyright 1994, American Chemical Society.

PF-127 hydrogels have been proved to many different applications, not only as a vehicle for DDS but also as an active agent for being able to modify multidrug resistant cancer cells. The PF-127 binds with the plasma membrane of said cells affecting its fluiditation, induces inner mitochondrial membrane polarization, and depletes ATP, decreasing antiapoptotic defense.[26] Rheological properties put this compound as an eligible support material for 3D printing tissue for biomimetic scaffolds,[27] due to the thermoplastic nature and yield stress it exhibits in gel form. This last application is also derived from tissue engineering, where noninvasive methods, such an injectable scaffold, are also a main objective.[28] More concretely, it can be included in regenerations of cartilage,[29] bone,[30] and even accelerates wound healing.[31]

Some of the most novelty applications for this material may also include neuroregeneration of the peripheral nervous system, where PF-127 with PLGA semipermeable nanosized porous structure would serve as a nerve guide and would allow blood vessels to grow and supply nutrients to growing axons,[32] or gene therapy, where PF combined with polyethileneimine (PEI) and conjugated with cell-penetrating peptide to the DR5-receptor in cancerous cells was used as a biodegradable and nontoxic system which showed higher gene transfection to cancerous cells than PEI alone.[33]

Moreover, PF-127-based hydrogels can effectively deliver drugs while adhering to biological tissues and minimizing surface tension, which aids in tissue targeting and protects the drug from degradation.[34] However, PF-127 hydrogels often dissolve quickly in physiological fluids, limiting their residence time, stability, and mechanical strength.[35,36] These limitations can be addressed by structural modifications, such as incorporating conjugated nanoparticles or copolymers to enhance strength and

promote tumor-specific drug delivery.[37] For instance, Ju et al. achieved localized delivery of paclitaxel using PF-127 hydrogels modified with carboxymethyl chitosan, resulting in a 40% increase in drug retention at the tumor site through cross-linking with glutaraldehyde.[38] Interaction with some drugs (overall when they are hydrophobic) may cause changes in the micellization and gelation process, presenting a more resistant structure depending on the drug concentration. This was described by Wei et al. with Ibuprofen interpenetrating micelles and restricting their motion.[24] In this context, hydrophobic materials have been used to modify the PF-127 network and enhance its effectiveness.[39]

Thus, modifying PF-127 with additional copolymers can mitigate rapid drug release without compromising thermosensitivity or injectability.[40,41] Other approaches embed intelligent nanoparticles into the hydrogel matrix, enhancing drug targeting and providing resistance against rapid degradation. Examples include alginate (ALG) microparticles, which have shown 10 times slower drug release rates than PF-127 alone,[42] dendrimers like polyamidoamine, which increase drug loading efficiency and exhibit cytocompatibility and anticancer activity,[43,44] and liposomes, which improve bioavailability and prolong drug residence time in treatments like retinal drug delivery.[45]

Another strategy is to create micelle systems with other Pluronics or surfactants, such as Tween 80,[46] P105,[47] P123,[48,49] or PF-68, optimizing drug release profiles for biomedical applications.[21,50,51] Additionally, incorporating polysaccharides can stabilize micelles and improve gel network properties without increasing toxicity, as polysaccharides are inherently biocompatible and biodegradable.

In this context, Bhowmick et al. studied the integration of xanthan and guar gum with PF-127 for ophthalmologic use,[52] and Dewan et al. found that adding tamarind seed polysaccharide improved elasticity, reduced porosity, and increased diffusion rates.[53] Brambilla et al. explored PF-127 with various polymeric excipients, including xanthan gum (XG), carrageenan, and HPMC, correlating sol–gel transition temperature, viscosity, and drug release.[54] Lupu et al. demonstrated that adding xanthan gum,[55] κ-carrageenan, alginate, and gellan gum enhanced the hydrogel's elastic modulus and viscosity.[56] De Dios-Pérez et al. (2023) observed that adding gellan gum and cyclodextrin complexes increased the elastic modulus up to 15 kPa in optimized formulations.[57]

While many approaches have improved localized delivery, cytotoxicity, and stability, few focus on the structural modifications that optimize the hydrogel properties for controlled drug release. Therefore, this work investigates the implementation of polysaccharides with distinct structures to PF-127 to precisely tune its thermosensitive properties. Rheological studies examine how polysaccharide–PF-127 networks alter gelation temperature and control drug release, specifically for 5-fluorouracil (5-FU).

Four polysaccharides are tested: XG with a helical structure; ALG and gellan gum (GG) with linear structures (GG also exhibits branches); and levan (LEV), a fructose polysaccharide that forms nanoparticles via self-assembly in water. Finally, a mathematical model correlates hydrogel stability and drug release behavior, accounting for transport resistance in the matrix.[58]

This study establishes a methodology for enhancing PF-127 hydrogels through polysaccharide incorporation, creating thermosensitive systems with customed properties for precise drug release and gelation control.

2. Experimental Section

2.1. Materials

Poloxamer PF-127 (#G2443), 5-FU (#G2443) and the following polysaccharides: XG (#G1253) with an average molecular weight around 1000 kDa, alginic sodium salt from brown algae (#G2033) with an average molecular weight around 150 kDa and a mannuronic to guluronic acid ratio of ≈1.56, and GG as Gelzan CM Gelrite (#1910) low acyl, with an average molecular weight around 1000 kDa were all purchased from Sigma-Aldrich. For levan synthesis D(+)-sucrose pure, pharma grade of molecular weight 342.30 Da was purchased from PanReacc AppliChem, the levansucrase enzyme (fructosyltransferase 68A) from Creative Enzymes, and ethanol (98% w/v) from Honeywell.

2.2. PF-127 Hydrogel Synthesis

10 mL of distilled water was poured in a beaker and left stirring at 4 °C. Once the water reached this temperature, the PF-127 was slowly added to the water while stirring to prevent aggregates. This mixture was left stirring overnight at 4 °C for PF-127 to be completely dissolved and obtain a homogeneous liquid hydrogel solution. The concentrations of PF-127 in these solutions were 10, 20, or 30% w/v.

2.3. Levan Synthesis

For levan synthesis, a cell-free methodology was used (molecular weight of the obtaining levan around 2000 kDa) described in references.[59] The levansucrase enzyme was added (0.2 mg L^{-1}) to a water solution of sucrose (90 g L^{-1}) in an AFORA reactor of 250 mL at 37 °C. After 72 h, the reaction was stopped, and the polymer was isolated by adding three volumes of ethanol to the reaction mixture. This new mixture was left at −20 °C for 24 h so the polymer precipitation could be induced. Afterward, the mixture was taken to centrifugation, using a tube Falcon centrifuge 5804 from Eppendorf (Madrid, Spain) at 10 000 rpm during 10 min, so levan could be separated from the supernatant. Finally, the polymer was taken to lyophilization, in a freeze dryer Telstar LyoQuest (Barcelona, Spain), prior freezing (−85 °C for 5 min), at −55 °C and 0.005 bar for 24 h.

2.4. PF-127 and Polysaccharide Hydrogel Synthesis

For hydrogel solutions with added polysaccharides (XG, ALG, GG, LEV), the process was similar to the one previously described in Section 2.2, with the only difference that the PF-127 was now dissolved in a polysaccharide aqueous solution instead of distilled water. For these polysaccharide aqueous solutions of 10 mL, concentrations of 0.5% and 1.0% w/v of the polysaccharides were added to distilled water at room temperature, except from gellan

Table 1. Formulations of polysaccharides and PF-127 hydrogels.

Formulation	Hydrogel [% w/v]	Formulation	Hydrogel [% w/v]	Formulation	Hydrogel [% w/v]
1	10% PF	10	0.5% ALG + 10% PF	19	1.0% GG + 10% PF
2	20% PF	11	0.5% ALG + 20% PF	20	1.0% GG + 20% PF
3	30% PF	12	0.5% ALG + 30% PF	21	1.0% GG + 10% PF
4	0.5% XG + 10% PF	13	1.0% ALG + 10% PF	22	0.5% LEV + 10% PF
5	0.5% XG + 20% PF	14	1.0% ALG + 20% PF	23	0.5% LEV + 20% PF
6	0.5% XG + 30% PF	15	1.0% ALG + 10% PF	24	0.5% LEV + 30% PF
7	1.0% XG + 10% PF	16	0.5% GG + 10% PF	25	1.0% LEV + 10% PF
8	1.0% XG + 20% PF	17	0.5% GG + 20% PF	26	1.0% LEV + 20% PF
9	1.0% XG + 30% PF	18	0.5% GG + 30% PF	27	1.0% LEV + 30% PF

gum, which dilution was obtained at 85 °C, and stirred for 1 h on a heating and magnetic stirring plate Isotemp from Fisherbrand (Madrid, Spain). After this time, homogeneous polysaccharide solutions were achieved. In this context, **Table 1** indicates the compositions of the different formulations PF-127 with the polysaccharides.

Once the polysaccharide solutions were at room temperature (GG solution needed an extra step cooling down from 80 °C to room temperature), these were taken to the cold chamber and were left with stirring at 4 °C until this temperature was reached. After that, the PF-127 was added with the same concentrations and following the procedure in Section 2.2. Finally, all of the hydrogels presented transparency in both solution and gel state, except from the LEV ones, which presented turbidity due to their characteristic Tyndall effect.[59] This turbidity slightly increased with the LEV concentration. The hydrogel samples can be seen in Figures S1 and S2 in the Supporting Information.

2.5. Rheology

The rheometer used was an AR 1500ex model from TA instruments (Madrid, Spain), equipped with a 4 cm diameter aluminum plate and a 1 mm gap. The rheological analysis was performed once the solutions were fully prepared and taken back to room temperature. Samples of 1.5 mL of the hydrogel (in liquid state) were loaded on the peltier and geometry gap was set to 1 mm.[20,57,60,61] Also, a solvent trap was used in the rheological measurements in order to control water evaporation. This solvent trap used vacuum grease and lightweight, low-viscosity, nonvolatile machine oil placed in the surroundings of the flat geometry head.

Both temperature and frequency sweep tests (oscillatory analysis) were performed on the hydrogels. The main variables measured were the elastic or storage (G') modulus and the viscous or loss (G'') modulus, obtaining the gct and elasticity of the gel systems. For temperature sweep tests, the temperature range studied was from 15 to 45 °C with a 1 °C min^{-1} rate, as described.[62,63] Also a temperature 5 °C min^{-1} rate was used in order to study the poloxamer's hysteresis. Fixed variables were frequency (10 Hz) and strain percentage (0.2%) so that the hydrogel provided results within its linear viscoelastic region. For frequency sweep tests, the frequency range studied was 0.5–500.0 rad s^{-1}. Fixed variables were temperature (37 °C), so that measured gel properties were the ones at physiological conditions, and strain percentage (0.2%).

Temperature ramp static flow analyses (static analysis) were also performed. For this type of analysis, the measured variable was the viscosity of the hydrogel, which provided information about the sol–gel transition. Tests kept the same temperature range studied in the oscillatory analysis (15–45 °C). Temperature ranges took into account storage temperature, operating room temperature,[64] and physiological temperature. The fixed variable for this analysis was the shear rate at 50 s^{-1} in order to observe the MAC effect on viscosity.[20]

2.6. Synthesis of the Loaded Hydrogels

Hydrogels were loaded with the antimetabolite drug 5-FU following previous Sections 2.2 and 2.4. For these hydrogels, a 5-FU standard solution was added to the distilled water or polysaccharide aqueous solution once it was stirring at 4 °C and prior to adding PF-127. The final concentration of 5-FU was 50 ppm, since it was reported as the IC_{50} in MTT assays.[65]

Let it be noted that, although PF-127 was proven to improve drugs solubility in aqueous phases,[66] the 5-FU IC_{50} was lower than its saturated concentration in water and a higher amount of 5-FU might promote side effects if the formulation was administered.

2.7. Drug Release Experiments

For drug release experiments, 5 mL of the loaded synthesized hydrogels (liquid state at 25 °C) was weighed in a 35 mm diameter Petri dishes and taken to incubation at 37 °C for 30 min. This time enabled the samples to fully undergo the gelification process in the incubator EN025, Nuve Incubator (Ankara, Turkey). Afterward, the Petri dish was placed in a support inside a 100 mL beaker full of distilled water, on a heating and stirring plate at 37 °C and 100 rpm. This system was connected to the spectrophotometer Cary 60 UV–vis from Agilent Technologies (Santa Clara, CA, USA) via a probe that enabled continuous measurements of the bulk. The temperature was controlled as well via probe connected to the plate. The bulk was measured periodically by the spectrophotometer probe at 260 nm (peak of 5-FU detection) at a temperature of 37 °C.[65] An experimental diagram explaining all

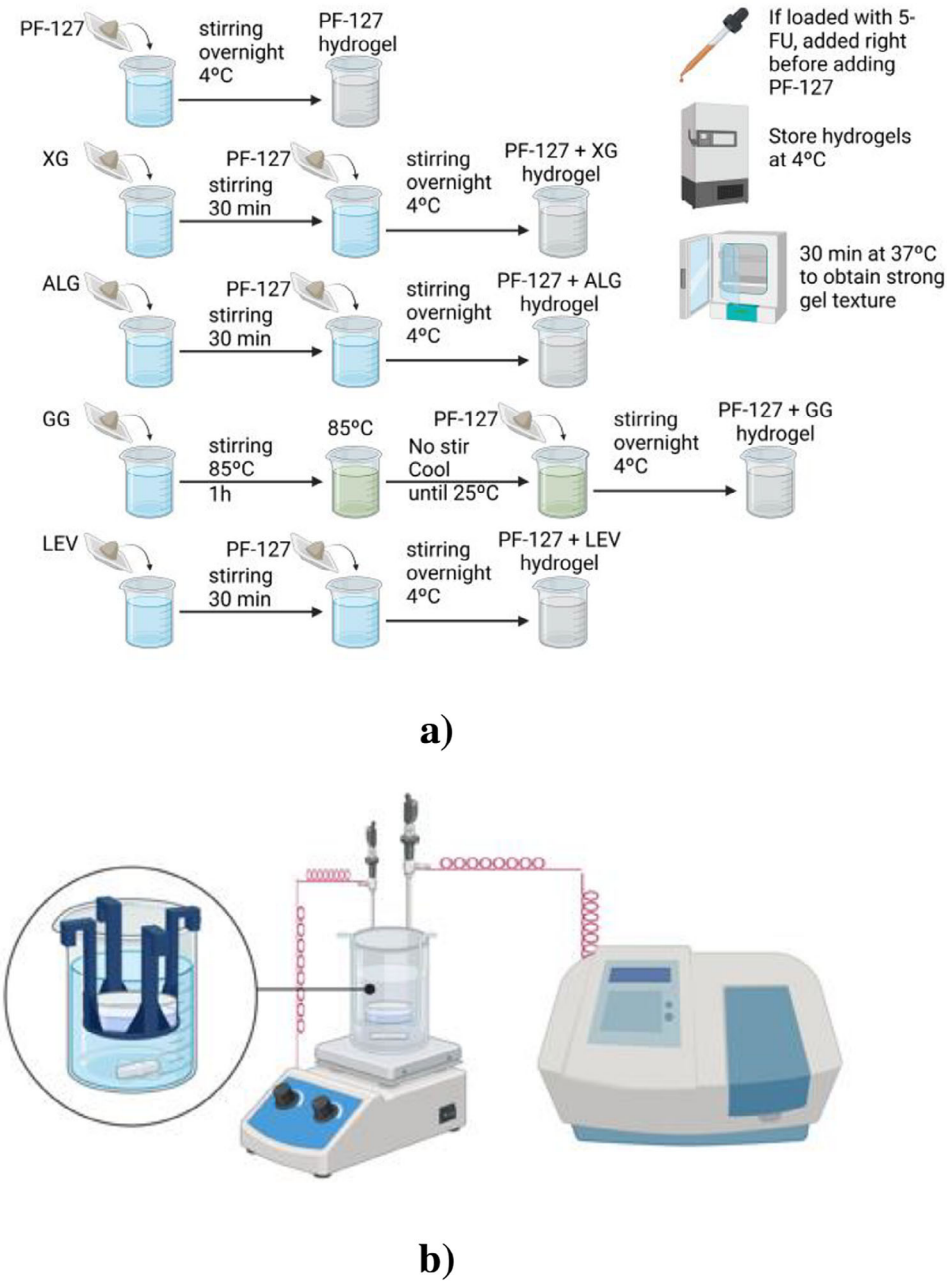

Figure 2. a) Experimental diagram of hydrogels synthesis processes, and b) scheme of the system setup for drug release experiments. This figure was created with BioRender.

of the hydrogels' synthesis and these experiments' setup is further illustrated in **Figure 2**.

2.8. Mathematical Modeling of the Drug Release Experiments

Drug release experimental results were fitted to a mathematical model in order to determine the constants values which explained the contribution of the polysaccharide and the PF-127 to the drug release. It was stated that the mass released of 5-FU was directly proportional to the degradation rate of the hydrogel,[57] and degradation rate was a function of the relative loss of mass of both polymers involved (W) and the fraction of chains released from the internal structure of the hydrogel (F).[58] This was expressed in the kinetic equation for these experiences Equation (1) below

$$M^{rel}{}_{5FU} = K_r \cdot \left(W_{PF} \cdot F_{PF} + W_X \cdot F_X\right) \quad (1)$$

being $M^{rel}{}_{5FU}$ the percentage of mass for 5-FU released, K_r the release constant, including all the resistances taking place in the transport phenomena (dimensionless), W and F the paremeters

explained before, and subtitles PF and X the reference to the compound being either the poloxamer (PF) or the polysaccharide, if any, respectively.

In order to estimate the F value, the model described another parameter P, a variable function of time according to Equation (1) and that depended on the degradation rate parameter, k_d. This parameter was further defined in Equation (2) shown below

$$P = 1 - \exp\left(k_d \cdot t\right) \tag{2}$$

being P the unitary fraction of degradation (dimensionless), k_d the degradation rate of the hydrogel chains (s^{-1}), and t the time (s). Once defined P, the released chains of both polymers of the system could now be calculated following Equations (3) and (4) shown below

$$F_X = \left(1 - (1 - P)^2\right)^N \tag{3}$$

$$F_{PF} = P^2 + P \cdot (1 - P) \cdot F_X \tag{4}$$

being N the erosion parameter (dimensionless, and ranges from 0 to 1 values). As a conclusion, three parameters would be estimated for this model: the release constant, the degradation rate, and the erosion parameter.

Parameter estimation was carried out by Solver add-in complement in Excel, where the relative error was the function that should be minimized by varying the three parameters mentioned above. This relative error definition followed the Equation (5) shown below

$$E_r = \frac{E_{abs}}{n} = \left|\frac{V_{th} - V_{exp}}{V_{th}}\right| \cdot \frac{100}{n} \tag{5}$$

being E_r and E_{abs} the relative and absolute errors, V_{th} and V_{exp} the theoretical and experimental values, respectively, and n the total number of experimental values collected during the experiences. All parameters of Equation (5) were dimensionless.

Furthermore, the Stokes–Einstein equation was also discussed in order to relate the diffusion coefficient/bulk diffusion and the viscosity of the hydrogels. This equation was shown below as Equation (6)

$$D = \frac{k_B \cdot T}{6\pi\mu R_0} \tag{6}$$

being D the diffusion coefficient ($m^2\ s^{-1}$), k_B the Boltzmann's constant (5.67×10^{-8} W m^{-2} K^{-4}), T the temperature (K), μ the solvent viscosity (Pa s), and R_0 the solute's radius (m).

3. Results and Discussion

3.1. Rheological Results

First, the rheological characterization of the hydrogels is presented evaluating parameters such as gct (which is determined as the first temperature presenting gel behavior)[24] in the temperature sweep test, and values of the storage moduli in the frequency sweep tests. Gct is the studied parameter concerning hydrogel injectability and thermal response to room and tissue temperatures. Let it be noted that thermosensitivity needs to happen between 25 and 37 °C (gct between these values) in order for formulations to be eligible for injectability and filling properties.[35,58] This is why these two temperatures are marked in the rheological analyses graphs below.

Also, the MAC is studied through temperature ramp tests. MAC is defined as the aggregation which causes the phase transition from isotropical aqueous solution to the BCC solid-like structure with increasing temperature. This phase transition has been studied by many authors in references for Pluronics.[22,24,25,57] More concretely, this characterization of the MAC is described by Shriky et al.[20] Results are taken into account for deciding the best hydrogel systems, based on their elastic and viscous properties that depend on their formulation.

3.1.1. PF-127 Hydrogel System

The hydrogel based off of PF-127 alone was first studied and characterized by all the rheological tests explained in Section 2.5. The main results of the poloxamer concentrations at 10, 20, and 30% w/v (formulations 1 to 3) are illustrated in **Figure 3**.

Figure 3a shows the temperature sweep test (oscillatory flow analysis) results for 10, 20, and 30% w/v concentrations of PF-127 hydrogels. As it can be seen in this figure, hydrogels with concentrations higher than 10% w/v underwent gelation when the temperature increased. This was represented when the G' increased exponentially from unstable measurements at low values, below 10 Pa, until a stable gel region, reaching values higher than 10 and 30 kPa for formulations 2 and 3, respectively.

This analysis not only proved that PF-127 hydrogels needed a concentration higher than 10% w/v in order to be thermosensitive and reach a gel state (since formulation 1 never reached it), but also that this gelation process showed a lower gct (34 and 23 °C) and a higher elastic nature (G' of around 11 and 25 kPa) when the concentration of PF-127 increased (formulations 2 and 3). This confirms previous studies about the thermosensitivity of PF-127.[20,56] In addition, let it be noted that for formulations 2 and 3, the elastic nature was confirmed since the storage moduli prevailed over the loss moduli. This is shown in Figure S3a (Supporting Information). Moreover, another interesting data that could be considered are the temperature where the hydrogel starts transitioning from liquid to solid (T_{LTS}), found in the onset of the steep increase of the complex modulus (G^*). T_{LTS} values are shown in **Table 2**, and representation of this complex moduli can be found in Figure S9a (Supporting Information).

Moreover, additional measurements were performed in order to confirm their reproducibility, as shown in Figure S4a (Supporting Information). Also, the hysteresis cycle of the poloxamer was studied. A cooling stage was added and it showed that the system returned to a solution state in a solid-to-liquid transition temperature[66,67] around 17 °C as reported.[68] Besides, the hysteresis cycle breadth was proven to shrink when the heating and cooling rates were lowered, as well as proven with other Pluronics like F68.[66,67] These results can be seen in Figure S4b (Supporting Information). Moreover, expanding the temperature sweep to lower temperatures determines the cmt for F2 at ≈7.5 °C,

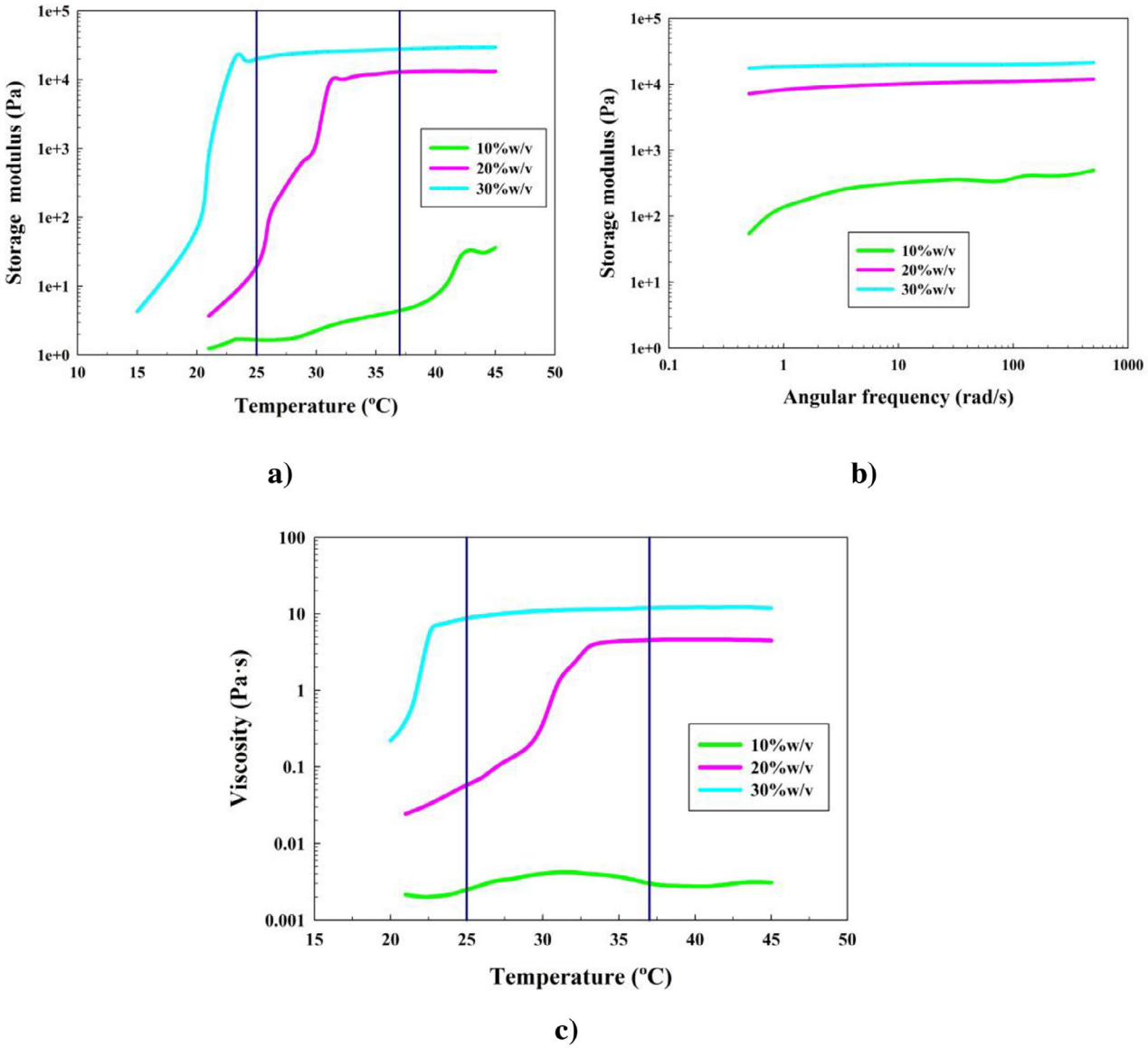

Figure 3. Rheological analyses of PF-127 hydrogels: a) temperature sweep oscillatory flow test, b) frequency sweep oscillatory flow test, and c) temperature ramp steady flow test.

corresponding to a minimum loss modulus value[66] when fitting experimental data to a polynomic trend, as shown in Figure S4c (Supporting Information). The cmt is found to be lower than other Pluronics like F68 at higher concentrations.[24] This might be due to the PEO/PPO ratio in the compounds.[25]

Figure 3b shows the angular frequency sweep of the PF-127 hydrogels at 37 °C. This test was performed in order to find a strong gel behavior of the systems specifically at physiological temperature. This fact was demonstrated since the elastic moduli of the systems were independent of the frequency. Also, these were always higher than the viscous moduli, exhibiting the elastic nature of the gel, as shown in Figure S3b (Supporting Information).

It was shown that this strong gel state was present at 37 °C for concentrations higher than 10% w/v, agreeing with previous results.[20,53,56] As stated before, when the PF-127 concentration increased (formulations 2 and 3), so did the elastic nature of the systems at any temperature, since elastic moduli values increased from 8 to 19 kPa. Moreover, the difference between elastic and loss moduli increased from 7 to 18 kPa, shown in Figure S3b (Supporting Information).

Figure 3c shows the 1 °C min^{-1} ramp temperature in static flow analysis. The heating rate was chosen as described.[62,63] It has been reported that this rate can affect the hysteresis cycle of Pluronic F68, but does not cause a significant difference (±1 °C) in the temperatures where the Pluronic F68 starts gelling or the gct.[66,67] This test is essential in order to understand the MAC that PF-127 exhibits. According to Figure 3c, three different stages were found. The first one (solution with liquid-like behavior) corresponds with a Newtonian formulation, since the viscosity values are low and only depend on the PF-127 concentration.

Table 2. Rheological analyses results, being T_{MAC} the temperature where MAC stabilizes at the start of the third stage.[20]

Form	Hydrogel [% w/v]	Rheology					
		Oscillatory flow				Steady flow	
		T_{sweep}		$Freq_{sweep}$		T_{ramp}	
		T_{LTS} [°C]	gct[°C]	G' [kPa]	$G' - G''$ [kPa]	T_{MAC} [°C]	μ [Pa s]
1	10% PF	No gelation process[a)]					
2	20% PF	26	34	8.63 ± 2.36	7.16 ± 0.77	34	4.53 ± 0.21
3	30% PF	19	24	19.40 ± 1.94	18.68 ± 0.90	24	11.21 ± 2.19
4	0.5% XG + 10% PF	No gelation process					
5	0.5% XG + 20% PF	No gelation process					
6	0.5% XG + 30% PF	24	28	8.89 ± 1.20	8.33 ± 0.26	No MAC[b)]	
7	1.0% XG + 10% PF	No gelation process					
8	1.0% XG + 20% PF	27	28	6.74 ± 2.45	6.12 ± 0.25	No MAC	
9	1.0% XG + 30% PF	20	24	11.49 ± 1.61	10.66 ± 0.87	No MAC	
10	0.5% ALG + 10% PF	No gelation process					
11	0.5% ALG + 20% PF	26	31	11.00 ± 3.07	9.74 ± 0.92	29	7.04 ± 1.67
12	0.5% ALG + 30% PF	18	23	10.31 ± 1.92	9.06 ± 0.75	22	13.15 ± 3.30
13	1.0% ALG + 10% PF	No gelation process					
14	1.0% ALG + 20% PF	26	31	10.76 ± 0.69	10.76 ± 0.69	29	7.18 ± 0.15
15	1.0% ALG + 30% PF	17	22	29.33 ± 1.64	28.36 ± 1.56	No MAC	
16	0.5% GG + 10% PF	No gelation process					
17	0.5% GG + 20% PF	26	32	15.88 ± 3.54	14.65 ± 0.58	32	6.98 ± 0.60
18	0.5% GG + 30% PF	18	25	10.31 ± 1.92	9.06 ± 0.75	No MAC	
19	1.0% GG + 10% PF	No gelation process					
20	1.0% GG + 20% PF	No gelation process					
21	1.0% GG + 30% PF	17	22	25.59 ± 5.60	23.21 ± 1.49	No MAC	
22	0.5% LEV + 10% PF	No gelation process					
23	0.5% LEV +20% PF	25	30	18.69 ± 2.46	17.31 ± 2.02	30	6.11 ± 0.86
24	0.5% LEV + 30% PF	19	23	8.38 ± 2.16	7.32 ± 2.47	No MAC	
25	1.0% LEV + 10% PF	No gelation process					
26	1.0% LEV+ 20% PF	25	28	18.09 ± 2.54	17.12 ± 1.55	30	6.39 ± 0.62
27	1.0% LEV + 30% PF	18	22	34.52 ± 2.60	32.98 ± 2.53	21	11.42 ± 3.04

[a)] No gelation process was observed in the temperature sweep oscillatory flow analysis; [b)] No MAC was observed due to unstable viscosity in temperature ramp steady flow analysis.

The gelation process starts in a second phase, where the viscosity starts being dependent and directly proportional to the temperature. Micelles start associating in the Q_2 phase since the water molecules evaporate. Finally, a more ordered structure and stable gel behavior is reflected in the third and final stage, where the viscosity becomes an independent variable from the temperature again.

Figure 3c also shows that an increase on the PF-127 concentration from formulation 2 to 3 affects the MAC, making the gel transition (when the third stage begins) decrease from 34 to 23 °C and the viscosity increase from 4 to 11 Pa s, respectively.

3.1.2. PF-127 and XG Hydrogels

In order to study the effect of the implementation of XG to the PF-127 hydrogels, the concentrations of 0.5 and 1.0% w/v of said polysaccharide were implemented to the system (formulations 4–9). The results obtained are shown in **Figure 4**.

Figure 4a,b represents the temperature sweep test for said formulations. The first observation was that the implementation of this polysaccharide never reached a gel state if the PF-127 concentration is 10% w/v (formulations 4 and 7). The other PF-127 concentrations underwent this gelation process. However, formulation 5 gel state did not show a clear stabilization, since the elastic modulus starts decreasing toward the end of the test. This is due to steric hindrance problems of few micelles linking with high ordered XG helix structure. These mentioned formulations were consequently discarded from future analyses.

Analyzing the XG implementation on the elastic moduli, it was observed that for formulations 6, 8, and 9, the storage moduli values were around 11, 7, and 16 kPa, respectively. This shows that increasing the XG concentration also increases the G' values.

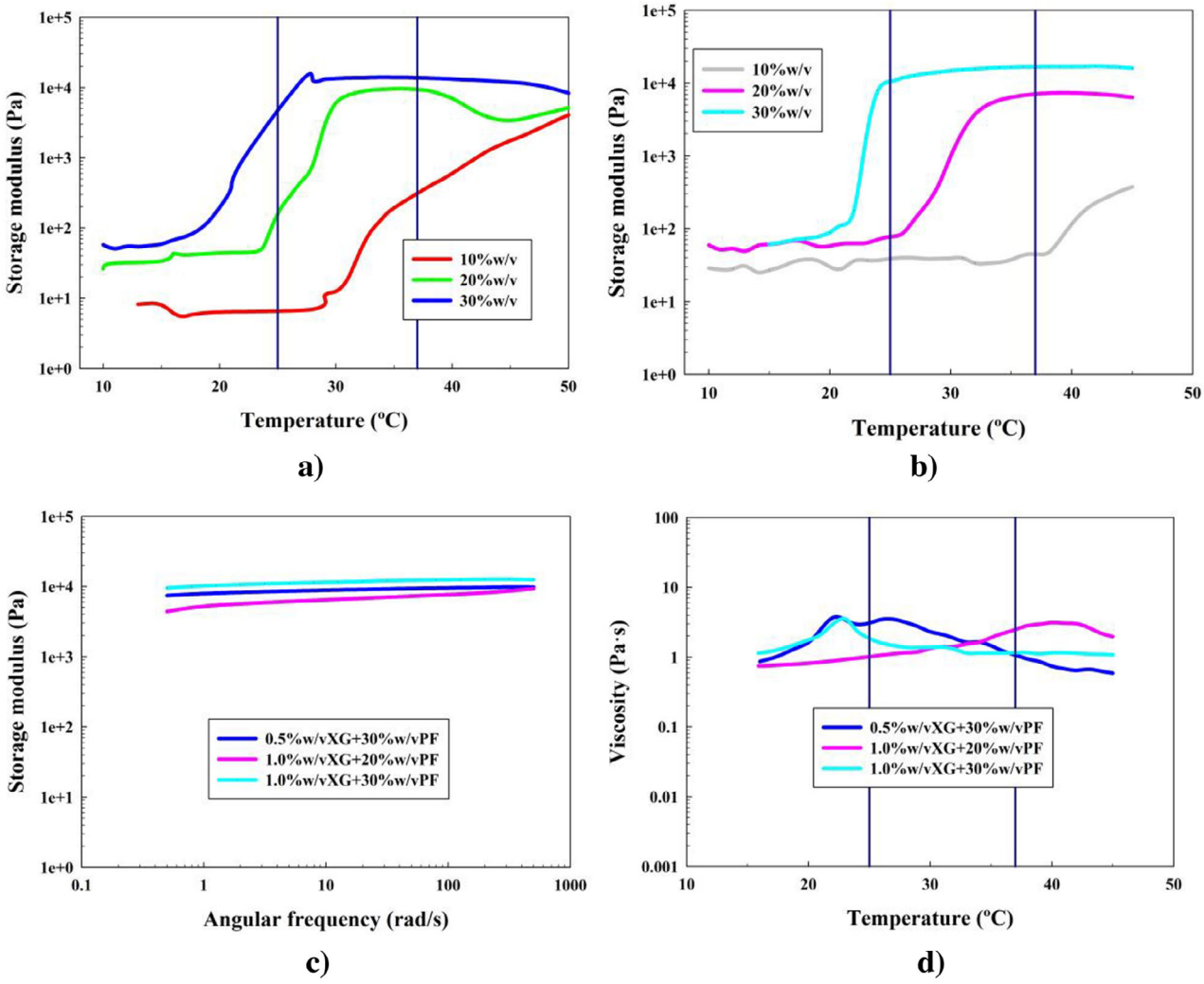

Figure 4. Rheological analyses of PF-127 and XG hydrogels: a) temperature sweep oscillatory flow test for 0.5% w/v XG, b) temperature sweep oscillatory flow test for 1.0% w/v XG, c) frequency sweep oscillatory flow test on gel formulations, and d) temperature ramp steady flow test on gel formulations.

However, these results obtained did not present any higher G' values than the hydrogels based off of PF-127 only. This means that XG implementation also caused difficulties to reach gel states as strong as PF-127 hydrogels. This was also shown with the gct values of these formulations, being 28, 28, and 24 °C for formulation 6, 8, and 9, respectively.

The stable gel state formulations shown in the temperature sweep test (formulations 6, 8, and 9) were taken to the frequency sweep test at 37 °C. In Figure 4c, this analysis showed a strong gel behavior for all formulations at this temperature. Storage moduli values reported were around 9, 7, and 12 kPa for formulations 6, 8, and 9, respectively. These results confirmed that the PF-127 concentration had a higher effect on gellation, since formulations with high XG concentration did not present higher G' values than those with low XG, or PF-127 alone hydrogels. Once again, XG implementation does not improve elastic nature of the hydrogels. Moreover, this elastic nature of XG and PF-127 hydrogels was confirmed in Figure S5a (Supporting Information), and G^* is shown in Figure S9b (Supporting Information).

Figure 4d shows the temperature ramp for the steady flow analysis. These results clearly showed that none of the formulations 6, 8, or 9 showed the MAC zones compared to PF-127 alone, since there is never a gel state stabilization. In this context, XG is a helicoidal polysaccharide,[69] which has a complex helix 3D structure that, according to the results, is difficult to coexist with the micelles present as colloids in the liquid bulk of the aqueous solution. This means that, as the temperature increased, the micelles started associating among them, increasing the viscosity but ended collapsing at the fixed shear rate of the static flow experiments, as shown in Figure 4d.[70] Therefore, a gel was formed with an internal structural disorder that provided the system with low viscosity values.

3.1.3. PF-127 and ALG Hydrogels

For the polysaccharide ALG, the rheological analyses are the ones shown in **Figure 5** (formulations 10–15).

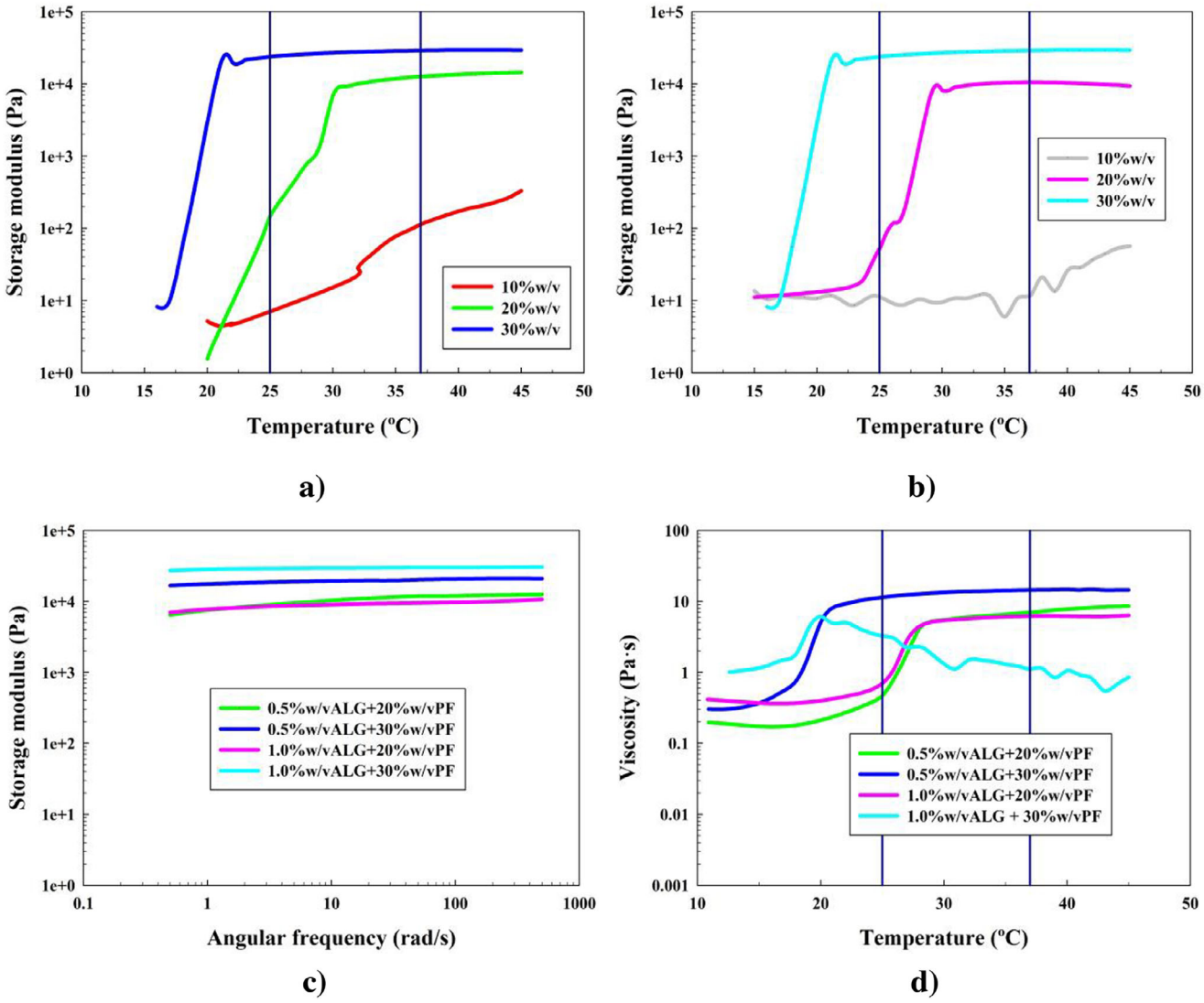

Figure 5. Rheological analyses of PF-127 and ALG hydrogels: a) temperature sweep oscillatory flow test for 0.5% w/v ALG, b) temperature sweep oscillatory flow test for 1.0% w/v ALG, c) frequency sweep oscillatory flow test on gel formulations, and d) temperature ramp steady flow test on gel formulations.

Figure 5a,b shows the results for all formulations 10–15 of the hydrogels in the temperature sweep tests. As it can be seen, once again, it was confirmed that for low concentrations of PF-127 (10% w/v, formulations 10 and 13), the gelation process was non-viable, no matter the ALG concentration added. However, the rest of the other formulations showed an efficient gelation process.

For this case, the gcts were 31 and 23 °C for formulations 11 and 12, and 31 and 22 °C for formulations 14 and 15, respectively. For this polysaccharide, only the increasing PF-127 concentration established an acceleration in the gelation process.

Moreover, the G' values were found to be equal or higher than the ones for PF-127 hydrogels. It was shown, for a 20% w/v PF-127 concentration, that ALG effect was more visible in its lower concentration (formulation 11), since its G' value does not promote with increasing ALG concentration.

These four formulations were taken to frequency sweep tests in order to confirm the strong gel behavior at the physiological temperature of 37 °C. Test results in Figure 5c first confirmed the strong gel behavior. The G' values were 11, 19, 11, and 29 kPa for formulations 11, 12, 14, and 15, respectively. First, these G' values were shown to be higher than the ones for PF-127 hydrogels, confirming the positive effect of ALG implementation.

As it can be seen, for a 20% w/v of PF-127 concentration, the alginate addition promoted the storage modulus value independently of its concentration, suggesting that lower ALG concentration was optimal for this PF-127 concentration.

Besides, when it came to considering the difference between the storage and loss moduli, the reported values were around 9, 18, 11, and 28 kPa, respectively. These are represented with their G'' in Figure S6 (Supporting Information) and G^* is shown in Figure S9c (Supporting Information). For ($G' - G''$) values, the ALG effect was more visible. When increasing ALG concentration, so did the elastic nature of the gels. This was also due to the elastic nature that ALG solutions have as well.[71]

Figure 5d shows the ramp temperature with steady flow analysis. First, formulation 15 clearly showed that the micelles are not stable and collapse at the fixed shear rate. The rest of the formulations did show a successful MAC. On the other hand, it was also observed a big difference in the gel stabilization temperatures when increasing PF-127 concentration, being these 29 °C for both formulations 11 and 14, and 22 °C for formulation 12. ALG hydrogels also reached higher viscosity values of 7, 13, and 7 Pa s, greater than the ones of PF-127 hydrogels. Moreover, it was shown that increasing ALG concentration did increase the viscous properties and confers the structure more strength toward external deformation forces. Finally, regarding formulation 12 gct, it is shown that the gelation occurs at lower temperatures than room temperature (25 °C).

In these systems, the PF-127 hydrophilic blocks (PEO) tend to mainly form hydrogen bonds with other functional groups with hydrogen in them (mainly alcohols and carboxylic acids). In the alginate case, the carboxylic acid groups can easily tend toward these interactions, as well as other electrostatic interactions.[71,72] The PF-127 and alginate system has been reported to form mesh macrostructures that increase their size when the PF-127 concentration does. Basically, the pluronic micelles are organized in cubic domains and induce the distortion of alginate chains.[73] Following this, different size meshes coexist in a nonhomogeneous spatial distribution of the micelles in the polymeric network, as long as the PF-127 concentration exceeds the value of 10% w/v, as shown in the results. The micelles organize into dense aggregates in which packing increases with the PF-127 concentration.[74] This also explains why the PF-127 concentration was more determinant in the experimental results in Figure 5d. For PF-127 formulations 11 and 14, the ones with 20% w/v PF, are the ones in which structure is potentially compatible for the application.

3.1.4. PF-127 and GG Hydrogels

The same procedure was followed to study GG implementation to the PF-127 hydrogels (formulations 16–21). The rheological analyses are shown in **Figure 6**.

First, looking at the temperature sweep tests in Figure 6a,b, it was once again proven that GG was not an exception for low concentrations (10% w/v) of PF-127 to undergo the gelation process. Moreover, for formulation 20, this process never occurred as well. Thus, we could first state that high concentrations of GG were not able to show the gelation process, since probably the branched and more spatially complex structure of the GG caused a collapse in the hydrogel structure.[75]

For the rest of the formulations, this gelation process was observed. The gcts were 32, 25, and 22 °C, for formulations 17, 18, and 21, respectively. All of these results did not present a significant increase when comparing with the PF-127 hydrogels. Therefore, GG did not interrupt the PF-127 gelation process, but surely did not promote it.

Results for the frequency sweep test in Figure 6c at 37 °C showed strong gel behavior for all the potential formulations. Storage moduli values were around 16, 10, and 25 kPa, which did not imply a significant difference for formulation 21 compared to formulation 3 (without polysaccharides). However, for formulation 17, it was found that the gel had significantly improved elastic properties compared to formulation 2, showing higher storage modulus value, and a higher difference between this one and the viscous one, around 15 kPa. This can be seen in Figure S7 (Supporting Information) and G^* is shown in Figure S9d (Supporting Information).

Figure 6d shows the temperature ramp steady flow test. As it can be seen, only the formulation 17 was able to reach the stabilization of its viscosity at a value close to 7 Pa s, greater than PF-127 hydrogel viscosity, and similar to the ones reported in the ALG systems.

In these formulations, the PF-127 also interacts via hydrogen bonds, with its strength increasing when the polysaccharide concentration does too. However, if the concentration increased from 0.5% w/v, the GG and its structure interfered with the PF-127 network making it unstable and collapsing the MAC at the fixed shear rate in Figure 6d.[75]

3.1.5. PF-127 and LEV Hydrogels

The last polysaccharide to be added to the system was LEV that was synthesized enzymatically from a sucrase solution, as described in previous sections (formulations 22–26). The results are the ones shown in **Figure 7**.

For LEV systems in Figure 7a,b, it was also confirmed that without enough PF-127 concentration, the gelation mechanism did not happen (formulations 22 and 25). There was also an exception concerning formulations 23 and 24, where the increasing PF-127 concentration caused a negative effect on the elastic modulus of the system. This can be seen in Figure 7a.

Nonetheless, the gel state was efficiently achieved for formulations 23, 24, 26, and 27. The gcts for these were 30, 23, 28, and 22 °C, respectively. These results implied that, apart from the exception, LEV effect was shown positive, since the gcts were lowered when it was added. Moreover, it is shown that LEV implementation improved the desired elastic properties of the PF-127 hydrogels, comparing their G' values with G' from PF-127 hydrogels.

These formulations were taken to the fixed temperature 37 °C, and were analyzed by a frequency sweep test in Figure 7c, showing that all of the hydrogels had a strong gel behavior. Let it also be noted that formulations 23 and 24 overlap each other, regardless of the polysaccharide concentration (green and purple lines in Figure 7c). As previously said, the results for this PF-127 concentration were improved by LEV addition, but not its concentration increase. The elastic moduli values reported were around 19, 8, 18, and 34 kPa, respectively. For formulations 23 and 26, LEV concentration had the same effect, while for formulations 24 and 27, the LEV effect was clear and visible, reaching G' higher than 30 kPa for both high concentrations.

For all the cases, besides formulation 24, the LEV addition caused a clear improvement over the elasticity of the PF-127 hydrogels. Not only when it came to elastic moduli values but also the difference between this and the viscous ones, being around 17, 7, 17, and 33 kPa, respectively. G'' of the formulations can be seen in Figure S8 (Supporting Information) and G^* is shown in Figure S9e (Supporting Information).

Studying the MAC through the temperature ramp test in Figure 7d, it was seen that the formulation 24 failed to show

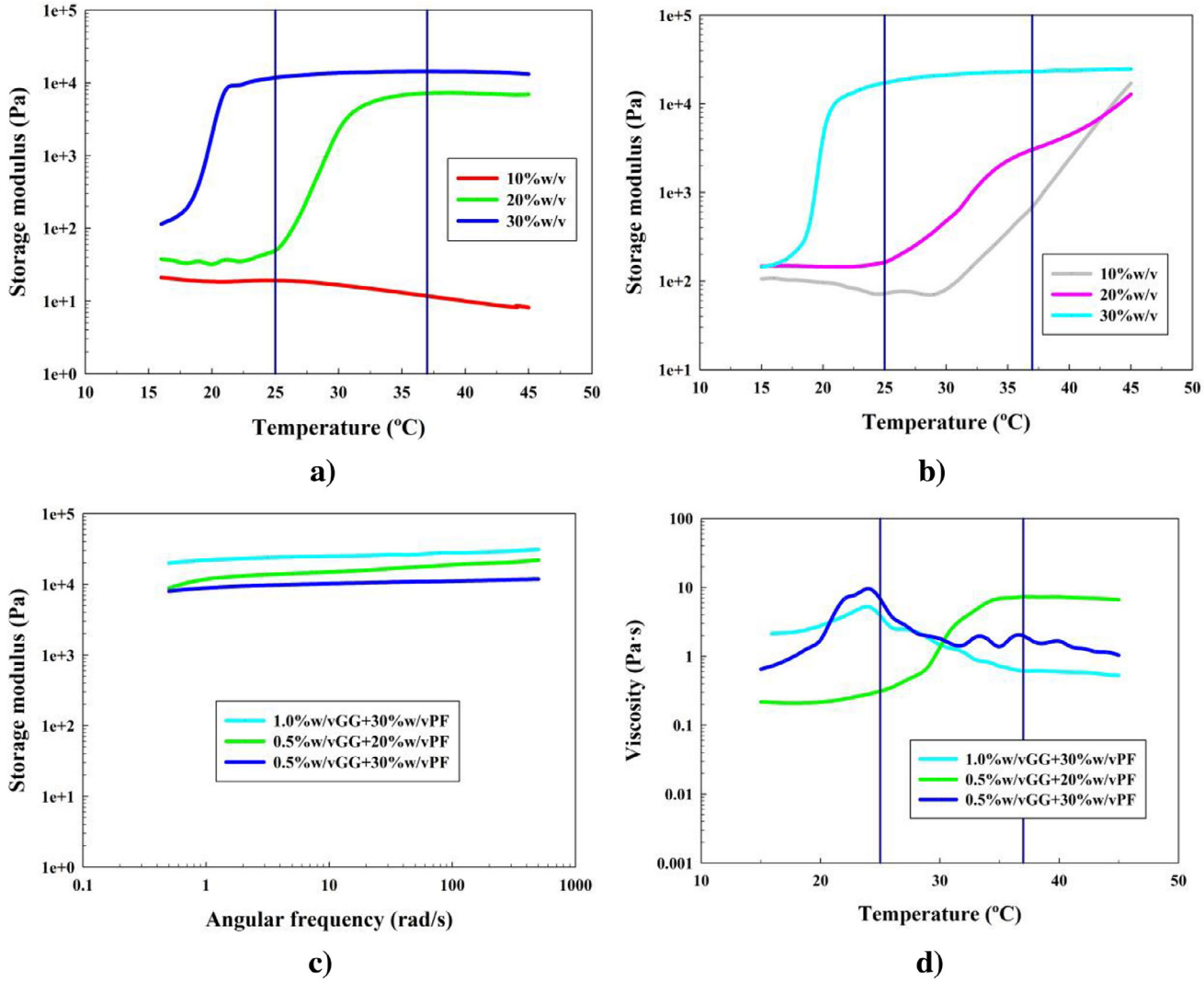

Figure 6. Rheological analyses of PF-127 and GG hydrogels: a) temperature sweep oscillatory flow test for 0.5% w/v GG, b) temperature sweep oscillatory flow test for 1.0% w/v GG, c) frequency sweep oscillatory flow test on gel formulations, and d) temperature ramp steady flow test on gel formulations.

a stable MAC at the studied shear rate. However, the rest of the formulations achieved this structure stabilization at temperatures of 30, 30, and 21 °C for formulations 23, 26, and 27. Reported viscosity values were around 6, 7, and 11 Pa s, respectively. These values were once again higher than the ones reported in PF-127 hydrogels, but the lowest of all polysaccharide systems. In order to explain the structure collapse of the formulation 24, it is important to take into account that levan is a self-assembly polysaccharide constituted of fructose units (—OH groups for hydrogen bonds), that forms nanoparticles inside the PF-127 micellar network. The addition of the nanoparticles explains why, if there was not enough PF-127 concentration, this ordered structure can collapse with high concentrations of LEV at a fixed shear rate, as shown in Figure 7d.[37] However, for formulations 23 and 26, both concentrations of LEV present the desired characteristics. Finally, observing the gct, it was possible to affirm that the formulation 27 had a gel state at room temperature.

It is therefore shown that the LEV effect highly improved the elastic nature of the hydrogels, since LEV is a self-assembly polysaccharide that does not present any complex structure to collapse the MAC. Besides, it also improved viscous properties, overall with higher concentrations, since more concentration means more viscosity taken by the hydrogel matrix to be more resistant against flow.

3.1.6. Selection of Optimal Formulations for Drug Release Experiments

Taking into account all the results obtained by the rheological analyses, Table 2 summarizes the final results for all formulations.

It is important to emphasize that for its use after a tumor resection, a strong gel has to be obtained at the physiological temperature (37 °C). This formulations need to present the MAC (ob-

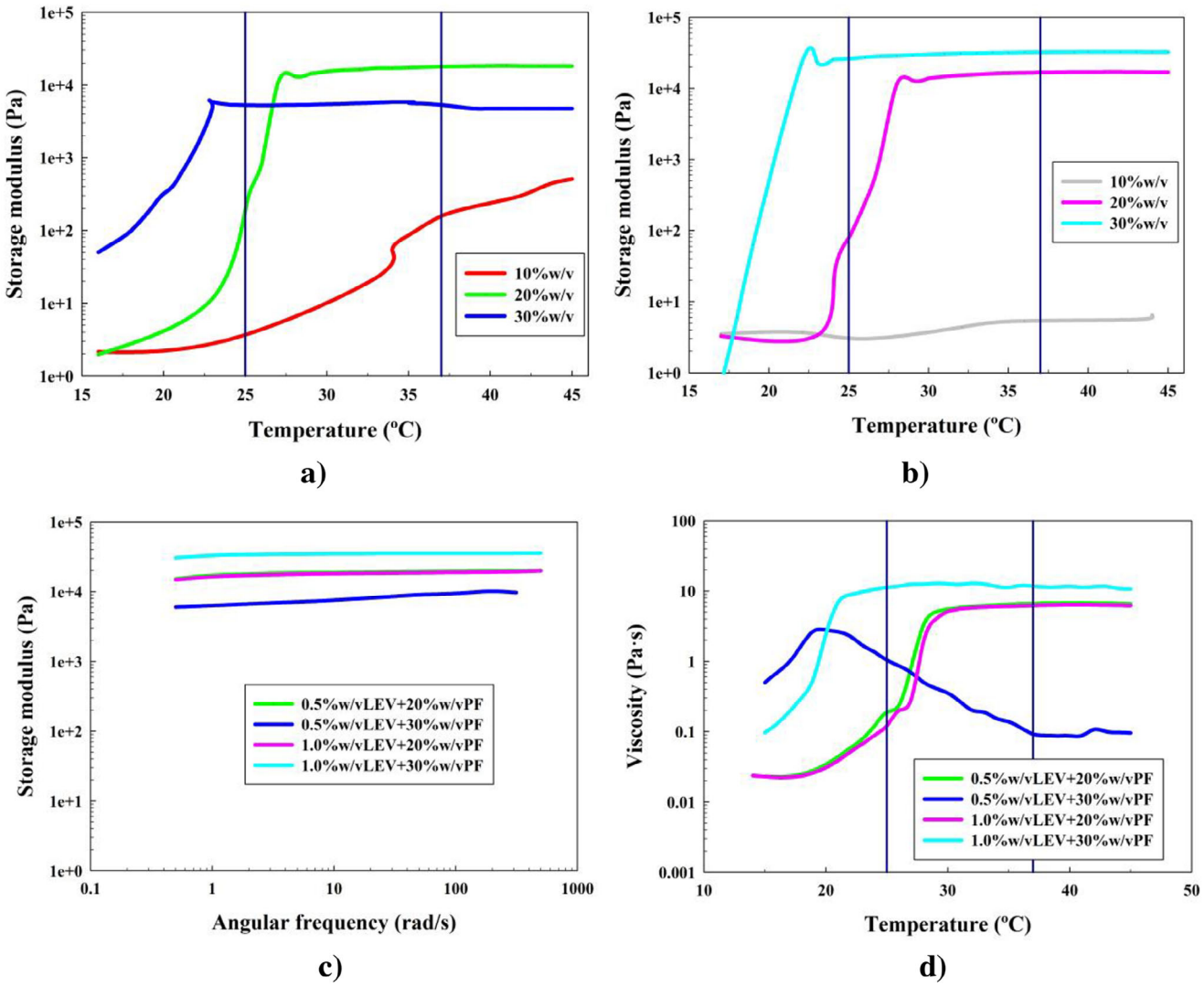

Figure 7. Rheological analyses of PF-127 and LEV hydrogels: a) temperature sweep oscillatory flow test for 0.5% w/v LEV, b) temperature sweep oscillatory flow test for 1.0% w/v LEV, c) frequency sweep oscillatory flow test on gel formulations, and d) temperature ramp steady flow test on gel formulations.

served in the temperature ramp steady flow analyses), reaching a stable higher viscosity once the gel state is achieved. It is also essential to present liquid state and aqueous solution behavior at room temperature (25 °C) in order to be injectable.[41] These characteristics must be studied through the understanding of interaction between the polysaccharides and the PF-127 hydrogel network.

Consequently, the potential formulations that were considered as potential DDS for the application mentioned were: 20% w/v PF-127, 0.5% and 1.0% w/v ALG with 20% w/v PF-127, 0.5% w/v GG with 20% w/v PF-127, and 0.5% and 1.0% w/v LEV with 20% w/v PF-127 (2, 11, 14, 17, 23, and 26, respectively).

3.2. Drug Release Experiments

All of these selected hydrogel systems were then loaded as described in Section 2.6 with a 5-FU concentration of 50 ppm, and then, the drug release experiments were performed as described in Section 2.7. Results for these experiments are shown in both **Figure 8** and **Table 3** below.

As it can be seen in Figure 8 and Table 3, for every system with any implemented polysaccharide at any concentration, the drug release was highly delayed, proving the point that polysaccharide structural implementation improved rheological properties and suits the hydrogels better for the desired application.[35] The PF-127 alone hydrogel presented a t_{10} lower than 1 min, t_{50} of 16 min, and t_{100} of 87 min. However, with polysaccharide structural effects, these times were delayed to 5–30 min for t_{10}, 70–145 min for t_{50}, and 260–440 min for t_{100}. This implied a minimum delay of 173 min (198% delay from PF-127 hydrogel) and a maximum delay of 353 min (405% delay from PF-127 hydrogel). Therefore, it can be stated that polysaccharides implemented systems contributed from double to quadruple the drug release time of the PF-127 hydrogels.

Table 3. Drug release studied parameters, being t_{10}, t_{50}, and t_{100} the times where 10%, 50%, and 100% of the drug concentration was released, respectively.

Form	Hydrogel [% w/v]	t_{10} [min]	t_{50} [min]	t_{100} [min]	G' [kPa]	Viscosity [Pa s]
2	20% PF-127	<1	16	87	8.63 ± 2.36	4.53 ± 0.21
11	0.5% ALG + 20% PF-127	9	81	315	11.00 ± 3.07	7.04 ± 1.67
14	1.0% ALG + 20% PF-127	31	145	440	11.49 ± 1.83	7.18 ± 0.15
17	0.5% GG + 20% PF-127	12	96	430	15.88 ± 3.54	6.98 ± 0.60
23	0.5% LEV + 20% PF-127	5	70	260	18.69 ± 2.46	6.11 ± 0.86
26	1.0% LEV + 20% PF-127	10	86	335	18.09 ± 2.54	6.39 ± 0.62

Systems exhibiting prolonged drug release correlated with higher viscosities rather than elevated G' values. This phenomenon is attributed to the structural characteristics of the polysaccharides and their interactions with PF-127 via hydrogen bonds.

Among the polysaccharides studied, LEV demonstrated the shortest drug release times, primarily due to its self-assembly organization. This configuration forms a lower pore interconnected and higher elastic, but more permeable gel matrix. In drug release experiments, water permeated the structure, leading to an easier dissolution of the micelles. The distilled water established hydrogen bonds with the network compounds, promoting disaggregation into colloids, accelerating its drug release.

Rheological analysis further supports this explanation, as LEV exhibited the lowest viscosity among the polysaccharide-based gels (observed in temperature ramp tests). Although LEV hydrogels were the most elastic systems, their viscous properties were the weakest. This indicated that its ability to resist against external stresses was lower than the other formulations, resulting in faster disaggregation. However, higher levan concentrations increased the system viscosity, enhancing resistance and extending drug release times.

By contrast, alginate showed relatively slower drug release due to its linear structure. This linear structure limits water permeability and resists disaggregation due to spatial constraints. This is due to the alginate matrix, which is organized as chains entrapped within micelle domains, that forms more hydrogen bonds per polysaccharide unit. Consequently, while ALG did not exhibit an elastic modulus as high as LEV, it provided greater resistance to drug release.

This effect was also observed in the increased viscosity values in the temperature ramp test, showing higher values than PF-127 and LEV systems. Additionally, as the concentration of polysaccharide increased, so did the viscous properties and drug release time.

The addition of branches in GG introduces further structural complexity. However, this structural conformation can interfere with the PF-127 gel stabilization, which limited the GG concentrations to 0.5% w/v, as discussed earlier (see Sections 3.1.4 and 3.1.6).

In terms of drug release, GG performed better than ALG at the same concentration, due to its viscous properties. The structural complexity of GG created a denser, more tortuous matrix, reducing pore size and hindering water permeability more effectively than simpler polysaccharides at the same low concentration range.

Ultimately, the system with ALG yielded the best drug release results, as its higher concentration compensated for the structural GG structure. A similar trend was observed with LEV, which outperformed the GG system due to its higher concentration. Notably, higher drug release times order nearly correspond with higher viscosity (see Section 3.3 for model fittings).

Additionally, it has been demonstrated that the structural characteristics of these polysaccharides enhance the hydrogel matrix, resulting in increased elasticity, a more consistent gel state, and overall, greater viscosity and resistance against external stresses. Consequently, drug release times in these composite hydrogels are slowed to between half and a quarter of those in PF-127 hydrogels alone.

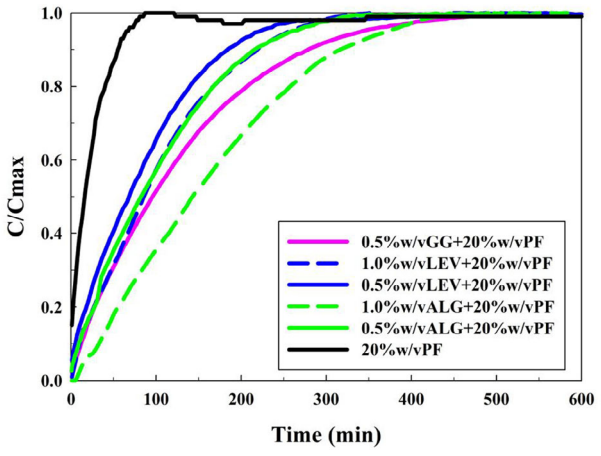

Figure 8. Drug release experiments with 5-FU-loaded PF-127 hydrogels.

3.3. Modeling and Parameter Estimation of Drug Release Experiments

As previously explained in Section 2.8, experimental results shown in Figure 8 were fitted to a model previously described. The results of this modeling are shown in **Table 4**.

Taking into account the previous results, after a first estimation it was decided to fix the K_r value of the formulation 2 to 1.000, since the release constant includes all of the resistances against the phenomena transport. This model stablishes that almost all of the release phenomenon is due to the hydrogel degradation, with added resistance when adding polysaccharides. These

Table 4. Drug release modeling.

Form	Formulation concentrations [% w/v]	k_d [s^{-1}]	N	K_r	E_{abs}	E_r [%]
2	20% PF-127	2.521	0.010	1.000	3.172	2.665
11	0.5% ALG and 20% PF-127	0.469	0.010	1.063	3.209	2.697
14	1.0% ALG and 20% PF-127	0.256	0.435	1.181	5.942	4.993
17	0.5% GG and 20% PF-127	0.416	0.027	1.063	1.345	1.130
23	0.5% LEV and 20% PF-127	0.667	0.010	1.003	3.556	2.988
26	1.0% LEV and 20% PF-127	0.512	0.101	1.038	4.099	3.445

PF-127 hydrogels were observed to not swell while studying their degradation process, with a good fitting to a model adapted to study this mechanism,[57] indicating the main contribution for degradation was the PF-127 and polysaccharide chain disaggregation. Also, let it be noted that the parameter N must be a positive value between 0 and 1, since erosion has an influence in the drug release mechanism.

As shown in Table 4, the degradation rate constant k_d decreased with increasing polysaccharide concentration, indicating a slower drug release. The highest k_d value was observed in the PF-127 alone hydrogel, presenting its weak resistance against degradation.[36] In fact, k_d was reduced until 10 times in the polysaccharide systems, confirming the necessity of their implementation to achieve controlled drug release. The most delayed release (lowest k_d) was observed in the formulation 14 (1.0% w/v ALG), attributed to the high concentration of the second-most structurally complex polysaccharide, showing the highest viscosity value, as discussed in Section 3.2.

Analyzing the k_d values from the highest (fastest degrading) to the lowest (slowest degrading), it is shown that the degradation rate strongly influenced the drug release order, and was closely correlated with the viscosity of each formulation. This suggests that increased viscosity correlates with a lower degradation rate, indicating that more viscous systems resist against external stresses more effectively, and thus delays drug release time.

The N factor, related to erosion, increased with polysaccharide concentration, and all values remained below 0.5, suggesting that the erosion process is predominantly controlled by water diffusion through the gel matrix (permeability). This permeability decreased with increasing polysaccharide concentrations, since the entangled structures hindered water permeation.

The highest N value was observed for the formulation 14, affirming that the most controlled release occurred in the structure that limited water permeability the most. Polysaccharide systems at 1.0% w/v showed the highest N values, confirming their increased resistance to permeation. The high N for formulation 26 (1.0% w/v LEV) may explain its slightly higher drug release time compared to formulation 23 (0.5% w/v ALG), despite showing a lower k_d value. On the other hand, the 0.5% w/v formulations 11 and 23 had the lowest N values, similar to PF-127. Additionally, the branched structure of the formulation 17 (0.5% w/v GG) hindered permeation more than simpler polysaccharide systems at the same concentration, explaining its lower k_d.

When observing the release constant K_r, it was noted that this parameter reflected both degradation and additional transport phenomena. All systems exhibited K_r values greater than 1.000, indicating diffusion as the gel degraded. Comparing the PF-127 to polysaccharide implemented systems, it was noted that polysaccharides reduced the gel porosity and increased the system tortuosity, consequently lowering effective diffusion compared to bulk diffusion.

This contribution to tortuosity was the highest in ALG, followed by GG, and finally LEV implemented systems, correlating with each polysaccharide structural organization. Moreover, it was observed that higher viscosity correlated with lower bulk diffusion, supporting more consistent and sustained release. For K_r, formulation 14 showed the highest resistance to drug release, also corresponding to the highest viscosity among all of the systems. This correlation between K_r and viscosity further supports the conclusion that hydrogel matrix

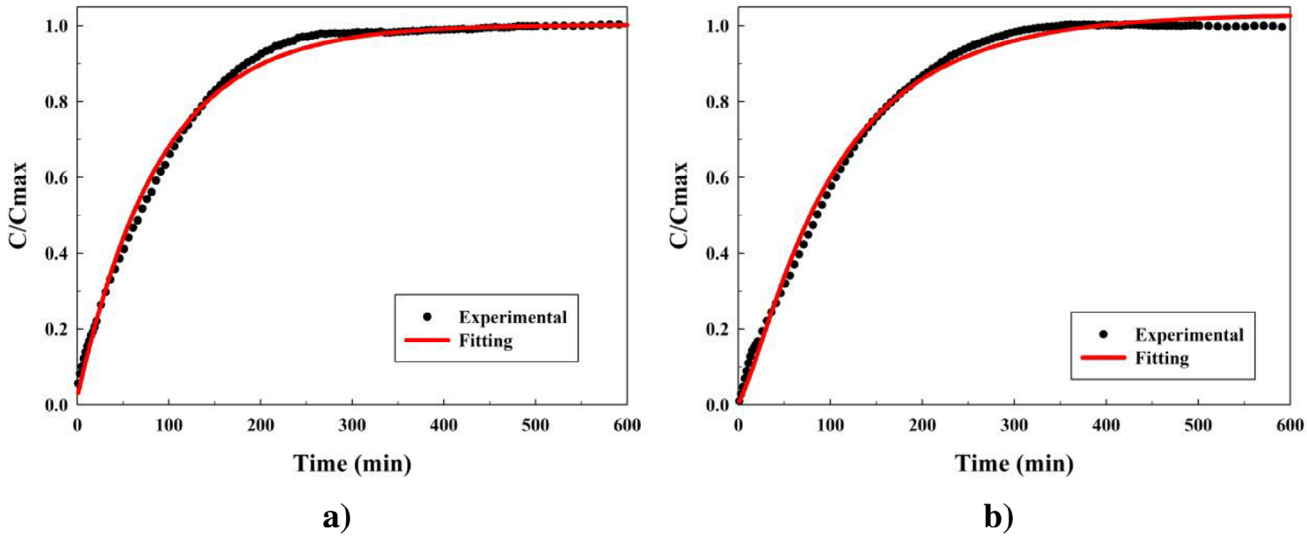

Figure 9. Graphical fittings to experimental drug release data for: a) formulation 17 and, b) formulation 14.

viscosity plays an essential role in controlling drug release kinetics.

Finally, commenting on the error values (E_r), as it can be seen in Table 4, all errors obtained are lower than 5.000%, which imply these models can be considered valid. A graphic proof of the models can be observed below in **Figure 9** showing the lowest (formulation 17) and the highest (formulation 14) errors (1.33% and 4.99%, respectively) obtained in the systems in Figure 9a,b, respectively. For the rest of the fittings, these can be seen in Figure S10 (Supporting Information).

4. Conclusions

This work examined the impact of the implementation of various polysaccharides to PF-127 hydrogels on their gelation behavior and control of 5-FU release. Analysis of gelation revealed that PF-127 concentrations above 10% w/v significantly increased the rheological properties of the system, enhancing elasticity, viscosity, and resistance to flow. Generally, the addition of polysaccharides increased the storage modulus and strengthened the gel structure at 37 °C, with higher viscosity values due to the supported MAC.

Six formulations were confirmed to undergo gelation between 25 and 37 °C, synthesizing consistent gels. These formulations included 20% w/v PF-127 alone, and in combination with 0.5% and 1.0% w/v ALG, 0.5% w/v GG, and 0.5% and 1.0% w/v LEV.

Drug release experiments with 5-FU-loaded hydrogels demonstrated that polysaccharide implementation significantly delayed release times by 2–4 times compared to the PF-127 hydrogel alone. Results indicated that higher polysaccharide concentrations and increased structural complexity promoted the systems viscosity and further delayed their drug release time.

Kinetic modeling of the drug release data confirmed polysaccharide and PF-127 chain disaggregation as the primary mechanism. Degradation rates, erosion factors, and release constants were calculated, showing that systems with higher viscosity, greater structural complexity, and prolonged drug release times exhibited lower degradation rates.

Finally, the release constant revealed that polysaccharide-implemented systems showed greater resistance to transport phenomena, resulting in reduced effective diffusion and enhanced viscosity. This release constant order correlated with viscosity trends from temperature ramp rheological analysis, confirming the relationship between viscosity and controlled release in the hydrogel systems.

Supporting Information

Supporting Information is available from the Wiley Online Library or from the author.

Acknowledgements

M.B.-L. wants to acknowledge the funds from the "Programa propio III de la Universidad de Salamanca: Ayudas para financiar contratos predoctorales de la Universidad de Salamanca cofinanciados por el Banco Santander" for his Ph.D. fellowship. The authors would like to express their gratitude to the Spanish Ministry of Science and Innovation for the financial support, research project: No. PID2022-1405990B-I00.

Conflict of Interest

The authors declare no conflict of interest.

Data Availability Statement

The data that support the findings of this study are available from the corresponding author upon reasonable request.

Keywords

drug release, mathematical model, PF-127, polysaccharides

Received: December 13, 2024
Revised: March 20, 2025
Published online: April 8, 2025

[1] N. Harbeck, F. Penault-Llorca, J. Cortes, M. Gnant, N. Houssami, P. Poortmans, K. Ruddy, J. Tsang, F. Cardoso, *Nat. Rev. Dis. Primers* **2019**, *5*, 66.
[2] R. N. Woodring, E. G. Gurysh, E. M. Bachelder, K. M. Ainslie, *ACS Appl. Bio Mater.* **2023**, *6*, 934.
[3] H. Daraee, A. Etemadi, M. Kouhi, S. Alimirzalu, A. Akbarzadeh, *Artif. Cells, Nanomed., Biotechnol.* **2016**, *44*, 381.
[4] W. H. De Jong, *Int. J. Nanomed.* **2008**, *3*, 133.
[5] Y. Li, J. Rodrigues, H. Tomás, *Chem. Soc. Rev.* **2012**, *41*, 2193.
[6] K. Y. Lee, D. J. Mooney, *Chem. Rev.* **2001**, *101*, 1869.
[7] D. Puppi, F. Chiellini, A. M. Piras, E. Chiellini, *Prog. Polym. Sci.* **2010**, *35*, 403.
[8] T. R. Hoare, D. S. Kohane, *Polym. J.* **2008**, *49*, 1993.
[9] C. Sandoval-Yañez, L. Escobar, C. A. Amador, *Processes* **2020**, *8*, 1331.
[10] M. Wang, M. Chen, W. Niu, D. D. Winston, W. Cheng, B. Lei, *Biomater. Res.* **2020**, *261*, 120301.
[11] S. Chatterjee, P. C. L. Hui, C. W. Kan, W. Wang, *Sci. Rep.* **2019**, *9*, 11658.
[12] X. Chen, M. Wang, X. Yang, Y. Wang, L. Yu, J. Sun, J. Ding, *Theranostics* **2019**, *9*, 6080.
[13] P. J. Rose Jaquilin, O. S. Oluwafemi, S. Thomas, A. O. Oyedeji, *J. Drug Delivery Sci. Technol.* **2022**, *72*, 103390.
[14] V. H. G. Phan, H. T. T. Duong, T. Thambi, T. L. Nguyen, M. H. Turabee, Y. Yin, S. H. Kim, J. Kim, J. H. Jeong, D. S. Lee, *Biomater. Res.* **2019**, *195*, 100.
[15] S. H. Kim, T. Thambi, V. H. G. Phan, D. S. Lee, *Carbohydr. Polym.* **2020**, *233*, 115832.
[16] T. M. D. Le, B.-K. Jung, Y. Li, H. T. T. Duong, T. L. Nguyen, J. W. Hong, C.-O. Yun, D. S. Lee, *Biomater. Sci.* **2019**, *7*, 4195.
[17] T. M. D. Le, H. T. T. Duong, T. Thambi, V. H. G. Phan, J. H. Jeong, D. S. Lee, *J. Biol. Macromol.* **2018**, *19*, 3536.
[18] A. C. Marques, P. C. Costa, S. Velho, M. H. Amaral, *Gels* **2023**, *9*, 593.
[19] J. Shi, L. Yu, J. Ding, *Acta Biomater.* **2021**, *128*, 42.
[20] B. Shriky, A. Kelly, M. Isreb, M. Babenko, N. Mahmoudi, S. Rogers, O. Shebanova, T. Snow, T. Gough, *J. Colloid Interface Sci.* **2020**, *565*, 119.
[21] N. U. Khaliq, J. Lee, S. Kim, D. Sung, H. Kim, *Pharm. J.* **2023**, *15*, 2102.
[22] P. Zarrintaj, J. D. Ramsey, A. Samadi, Z. Atoufi, M. K. Yazdi, M. R. Ganjali, L. M. Amirabad, E. Zangene, M. Farokhi, K. Formela, M. R. Saeb, M. Mozafari, S. Thomas, *Acta Biomater.* **2020**, *110*, 37.
[23] J. J. Escobar-Chavez, M. Lopez-Cervantes, A. Naik, Y. N. Kalia, D. Quintanar-Guerrero, A. Ganem-Quintanar, *J. Pharm. Pharmaceut. Sci.* **2006**, *9*, 339.
[24] D. Wei, L. Ge, R. Guo, *Colloids Surf., A* **2018**, *553*, 1.
[25] G. Wanka, H. Hoffmann, W. Ulbricht, *Macromolecules* **1994**, *27*, 4145.

[26] D. Y. Alakhova, *Mol. Pharmaceutics* **2014**, *11*, 2566.
[27] J. P. K. Armstrong, M. Burke, B. M. Carter, S. A. Davis, A. W. Perriman, *Adv. Healthcare Mater.* **2016**, *5*, 1724.
[28] P. Zarrintaj, M. Jouyandeh, M. R. Ganjali, B. S. Hadavand, M. Mozafari, S. S. Sheiko, M. Vatankhah-Varnoosfaderani, T. J. Gutiérrez, M. R. Saeb, *Eur. Polym. J.* **2019**, *117*, 402.
[29] D. Seol, M. J. Magnetta, P. S. Ramakrishnan, G. L. Kurriger, H. Choe, K. Jang, J. A. Martin, T.-H. Lim, *J. Biomed. Mater. Res., Part B* **2013**, *101*, 1508.
[30] A. Gigout, M. D. Buschmann, M. J. B. Jolicoeur, *Biotechnol. Bioeng.* **2008**, *100*, 975.
[31] J. Wu, J. Zhu, C. He, Z. Xiao, J. Ye, Y. Li, A. Chen, H. Zhang, X. Li, L. Lin, Y. Zhao, J. Zheng, J. Xiao, *ACS Appl. Mater. Interfaces* **2016**, *8*, 18710.
[32] S. H. Oh, J. H. Kim, K. S. Song, B. H. Jeon, J. H. Yoon, T. B. Seo, U. Namgung, I. W. Lee, J. H. Lee, *Biomaterials* **2008**, *29*, 1601.
[33] Z. Wu, S. Zhan, W. Fan, X. Ding, X. Wu, W. Zhang, Y. Fu, Y. Huang, X. Huang, R. Chen, M. Li, N. Xu, Y. Zheng, B. Ding, *Nano Res.* **2016**, *11*, 122.
[34] K. K. Jain, *Methods Mol. Biol.* **2020**, *2059*, 1.
[35] M. S. H. Akash, K. Rehman, *J. Controlled Release* **2015**, *209*, 120.
[36] C. He, S. W. Kim, D. S. Lee, *J. Controlled Release* **2008**, *127*, 189.
[37] W. I. Choi, Y. Hwang, A. Sahu, K. Min, D. Sung, G. Tae, J. H. Chang, *Biomater. Sci.* **2018**, *6*, 2627.
[38] C. Ju, J. Sun, P. Zi, X. Jin, C. Zhang, *J. Pharm. Sci.* **2013**, *102*, 2707.
[39] N. A. Di Spirito, N. Grizzuti, R. Pasquino, *Phys. Fluids* **2024**, *36*, 111302.
[40] D. S. Pellosi, I. R. Calori, L. B. de Paula, N. Hioka, F. Quaglia, *Mater. Sci. Eng.* **2017**, *71*, 1.
[41] A. González-Garcinuño, A. Tabernero, M. Blanco-López, E. Martín del Valle, S. Kenjeres, *Eur. J. Pharm. Sci.* **2024**, *203*, 106917.
[42] M. Cidade, D. Ramos, J. Santos, H. Carrelo, N. Calero, J. Borges, *Materials* **2019**, *12*, 1083.
[43] Z. Gu, M. Wang, Q. Fang, H. Zheng, F. Wu, D. Lin, Y. Xu, Y. Jin, *Drug Dev. Ind. Pharm.* **2015**, *41*, 812.
[44] T. T. C. Nguyen, C. K. Nguyen, T. H. Nguyen, N. Q. Tran, *Mater. Sci. Eng., C* **2017**, *70*, 992.
[45] S. Blazaki, C. Tsika, M. Tzatzarakis, E. Naoumidi, A. Tsatsakis, C. Tsatsanis, M. K. Tsilimbaris, *Graefe's Arch. Clin. Exp. Ophthalmol.* **2017**, *255*, 2375.
[46] Y. Yang, J. Wang, X. Zhang, W. Lu, Q. Zhang, *J. Controlled Release* **2009**, *135*, 175.
[47] Y. Chen, W. Zhang, J. Gu, Q. Ren, Z. Fan, W. Zhong, X. Fang, X. Sha, *Int. J. Pharm.* **2013**, *452*, 421.
[48] W. Zhang, Y. Shi, Y. Chen, S. Yu, J. Hao, J. Luo, X. Sha, X. Fang, *Eur. J. Pharm. Biopharm.* **2010**, *75*, 341.
[49] W. Zhang, Y. Shi, Y. Chen, J. Ye, X. Sha, X. Fang, *Biomaterials* **2011**, *32*, 2894.
[50] P. D. Kelishady, E. Saadat, F. Ravar, H. Akbari, F. Dorkoosh, *Pharm. Dev. Technol.* **2015**, *20*, 1009.
[51] Y. Chen, W. Zhang, Y. Huang, F. Gao, X. Sha, X. Fang, *Int. J. Pharm.* **2015**, *488*, 44.
[52] M. Bhowmik, P. Kumari, G. Sarkar, M. K. Bain, B. Bhowmick, Md. M. R. Mollick, D. Mondal, D. Maity, D. Rana, D. Bhattacharjee, D. Chattopadhyay, *Int. J. Biol. Macromol.* **2013**, *62*, 117.
[53] M. Dewan, K. Dutta, D. Rana, A. Basu, A. Bhattacharya, A. Adhikary, D. Chattopadhyay, *New J. Chem.* **2020**, *44*, 15708.
[54] E. Brambilla, S. Locarno, S. Gallo, F. Orsini, C. Pini, M. Farronato, D. V. Thomaz, C. Lenardi, M. Piazzoni, G. Tartaglia, *Polymers* **2022**, *14*, 3624.
[55] A. Lupu, M. Bercea, M. Avadanei, L. M. Gradinaru, L. E. Nita, V. R. Gradinaru, *Macromol. Mater. Eng.* **2024**, 2400341, https://doi.org/10.1002/mame.202400341.
[56] A. Lupu, I. Rosca, V. R. Gradinaru, M. Bercea, *Polymers* **2023**, *15*, 355.
[57] I. de Dios-Pérez, A. González-Garcinuño, A. Tabernero, M. Blanco-López, J. A. García-Esteban, V. Moreno-Rodilla, B. Curto, P. Pérez-Esteban, E. M. Martín del Valle, *Eur. J. Pharm. Sci.* **2023**, *191*, 106618.
[58] J. Xu, E. Feng, J. Song, *J. Am. Chem. Soc.* **2014**, *136*, 4105.
[59] A. González-Garcinuño, A. Tabernero, G. Marcelo, V. Sebastián, M. Arruebo, J. Santamaría, E. M. Martín del Valle, *Int. J. Biol. Macromol.* **2019**, *137*, 62.
[60] Y.-I. Chung, S.-Y. Lee, G. Tae, *Colloids Surf., A* **2006**, *284*, 480.
[61] G. E. Newby, I. W. Hamley, S. M. King, C. M. Martin, N. J. Terrill, *J. Colloid Interface Sci.* **2009**, *329*, 54.
[62] A. P. Constantinou, V. Nele, J. J. Doutch, J. S. Correia, R. V. Moiseev, M. Cihova, D. C. A. Gaboriau, J. Krell, V. V. Khutoryanskiy, M. M. Stevens, T. K. Georgiou, *Macromolecules* **2022**, *55*, 1783.
[63] O. Kontogiannis, D. Selianitis, D. R. Perinelli, G. Bonacucina, N. Pippa, M. Gazouli, S. Pispas, *Int. J. Mol. Sci.* **2022**, *23*, 13814.
[64] F. P. Ellis, *Br. J. Ind. Med.* **1963**, *20*, 284.
[65] C. Karthika, R. Sureshkumar, D. V. Sajini, G. Md. Ashraf, Md. H. Rahman, *Environ. Sci. Pollut. Res.* **2022**, *29*, 63202.
[66] N. A. Di Spirito, N. Grizzuti, M. Casalegno, F. Castiglione, R. Pasquino, *Int. J. Pharm.* **2023**, *644*, 123353.
[67] S. Costanzo, A. Di Sarno, M. D'Apuzzo, P. Renato Avallone, E. Raccone, A. Bellissimo, F. Auriemma, N. Grizzuti, R. Pasquino, *Phys. Fluids* **2021**, *33*, 043113.
[68] S.-Y. Lee, G. Tae, Y.-H. Kim, *J. Biomater. Sci., Polym. Ed.* **2007**, *18*, 1335.
[69] G. Sworn, in *Handbook of Hydrocolloids*, 3rd ed., (Eds: G. O. Phillips, P. A. Williams), Woodhead Publishing Series in Food Science, Technology and Nutrition, Woodhead Publishing, Sawston, England **2021**, p. 833.
[70] M. Suhail, I. Chiu, Y. Lai, A. Khan, N. S. Al-Sowayan, H. Ullah, P. C. Wu, *Gels* **2023**, *9*, 640.
[71] M. Blanco-López, A. González-Garcinuño, A. Tabernero, E. M. Martín del Valle, *Polymers* **2021**, *13*, 966.
[72] M. Blanco-López, A. Marcos-García, A. González-Garcinuño, A. Tabernero, E. M. Martín del Valle, *Polym. Adv. Technol.* **2024**, *35*, 6554.
[73] M. Abrami, I. D'Agostino, G. Milcovich, S. Fiorentino, R. Farra, F. Asaro, R. Lapasin, G. Grassic, M. Grassi, *Soft Matter* **2014**, *10*, 729.
[74] I. Frisman, D. Seliktar, H. Bianco-Peled, *Acta Biomater.* **2012**, *8*, 51.
[75] M. Dewan, G. Sarkar, M. Bhowmik, B. Das, A. K. Chattoapadhyay, D. Rana, D. Chattopadhyay, *Int. J. Biol. Macromol.* **2017**, *102*, 258.

